Computational vision systems for the detection of malignant melanoma

Ilias Maglogiannis[a*], Dimitrios I. Kosmopoulos[b]

[a]Univ. of Aegean, Dept. of Information and Communication Systems Engineering
83200 Karlovasi, Greece

[b]National Centre for Scientific Research ìDemokritosî,
Institute of Informatics and Telecommunications
15310 Aghia Paraskevi, Greece

Abstract

In the recent years computational vision-based diagnostic systems for dermatology have demonstrated significant progress. In this work, we review these systems by firstly presenting the visual features used for skin lesion classification and methods for defining them. Then we describe how to extract these features through digital image processing methods, i.e., segmentation, registration, border detection, color and texture processing). Then we present how to use the extracted features for skin lesion classification by employing artificial intelligence methods and heuristics, i.e., Discriminant Analysis, Neural Networks, Support Vector Machines. We finally compare these techniques in discriminating malignant melanoma tumors versus dysplastic naevi lesions.

KEYWORDS: Skin Lesion, Pattern Analysis, Melanoma, Dermoscopy, Discriminant Analysis, Neural Networks, Support Vector Machines.

1. Introduction

Malignant melanoma is among the most frequent types of skin cancer and one of the most malignant tumors. Its incidence has increased faster than that of almost all other cancers and the annual incidence rates have increased on the order of 3ñ7% in fair-skinned populations in recent decades (1). The advanced cutaneous melanoma is

[*] *Correspondence to* : Dr. Ilias Maglogoiannis University of the Aegean, Dept. of Information and Communication Systems Engineering, 83200 Karlovasi, Greece
Email: imaglo@aegean.gr, phone +30-2273-82239, fax +30-2273-82009, http://www.icsd.aegean.gr,

still incurable, but when diagnosed at early stages it can be cured without complications. However, the differentiation of early melanoma from other pigmented skin lesions is not trivial even for experienced dermatologists. The issue has attracted the interest of many researchers, who have developed systems for automated detection of malignant melanoma in skin lesions, which will be surveyed here.

The main design issues for a machine vision system for melanoma detection concern the image acquisition set up, the image processing and the classification methodology. More specifically the following questions have to be addressed:

1. How can we acquire good images?
2. How are the image features defined, i.e., what are we looking for?
3. How are these features detected in the image? (usually trivial for humans but non-trivial for machines).
4. Which are the proper features to use and how many are they? (feature selection).
5. How do we use the features to design the classifier for the specific task, i.e., what is the relative importance of each feature and what happens when contradictory features are detected?
6. How can we assess the performance of a classifier?

2. Materials and Methods

2.1 Image acquisition

The first step in machine vision-based expert systems involves the acquisition of the tissue digital image. The main techniques used for this purpose are the epiluminence microscopy (ELM or dermoscopy) and the image acquisition using still or video cameras. By placing a thin layer of oil on a lesion and then pressing a special hand-held microscope against the oil field on the patient's skin, ELM provides for a more detailed inspection of the surface of pigmented skin lesions and renders the epidermis translucent, making many features become visible. Recently new techniques have been presented, that use multispectral images. The chosen wavelengths interact preferentially with constituents of the skin and are able to reveal the structure of the skin lesion. An example is the work presented in (2).

The construction of systems with the ability to capture reliable and reproducible images of skin is rather challenging due to equipment and environmental constraints, such as image resolution, image noise, illumination, skin reflectivity and pose

uncertainty. The use of commercially available photographic cameras is quite common in skin lesion inspection systems, particularly for telemedicine purposes (3). However, the poor resolution in very small skin lesions, i.e., lesions with diameter of less than 0,5 cm, and the variable illumination conditions are not easily handled and therefore high-resolution devices with low-distortion lenses have to be used. However, the requirement for constant image colors, (necessary for image reproducibility) remain unsatisfied, as it requires real time, automated color calibration of the camera, i.e., adjustments and corrections to operate within the dynamic range of the camera and to measure always the same color regardless of the lighting conditions. The problem can be addressed by using video cameras that are parametrizable online and can be controlled through software (4), (5) at the price of higher complexity and costs.

2.2 Definition of features for detection of malignant melanoma

In this section we will examine the features, i.e., the visual cues that are used for melanoma detection. Similarly to the traditional diagnosis procedure, the computer-based systems look for features and combine them to characterize the lesion as malignant melanoma or dysplastic nevus. The features employed have to be measurable and of high sensitivity, i.e., high correlation of the feature with malignant melanoma and high probability of true positive response. Furthermore, the features should have high specificity, i.e., high probability of true negative response. Although in the typical classification paradigm both factors are considered important (a trade-off expressed by maximizing the area under the Receiver-Operating-Characteristic curve), in the case of malignant melanoma the suppression of false negatives (i.e., increase of true positives) is obviously more important.

In the conventional procedure, the following diagnostic methods are mainly used (6): (i) *ABCD rule* of dermoscopy (ii) *Pattern Analysis*; (iii) *Menzies* method; and (iv) *7-Point Checklist*. The features used for these methods are presented in the following. The *ABCD rule* investigates the *asymmetry* (A), *border* (B), *color* (C) (Figure 1), and *differential structures* (D) (Figure 2) of the lesion and defines the basis for a diagnosis by a dermatologist. More specifically:

- Asymmetry: The lesion is bisected by two axes that are positioned to produce the lowest asymmetry possible, in terms of borders, colors, and dermoscopic structures.

- Border: The lesion is divided into 8 pie-piece segments. Then it is examined if there is a sharp, abrupt cut-off of pigment pattern at the periphery of the lesion or a gradual, indistinct cut-off.
- Color: The number of colors present is determined. They may include: Light Brown, Dark Brown, Black, Red (red vascular areas are scored), White (if whiter than the surrounding skin), Slate-blue.
- Differential structures: The number of structural components present is determined, i.e., Pigment Network, Dots (scored if three or more are present), Globules (scored if two or more are present), Structureless Areas (counted if larger than 10% of lesion), Streaks (scored if three or more are present).

The *Pattern Analysis* method seeks to identify specific patterns, which may be global (Reticular, Globular, Cobblestone, Homogeneous, Starburst, Parallel, Multicomponent, Nonspecific) or local (Pigment network, Dots/globules, Streaks, Blue-whitish veil, Regression structures, Hypopigmentation, Blotches, Vascular structures).

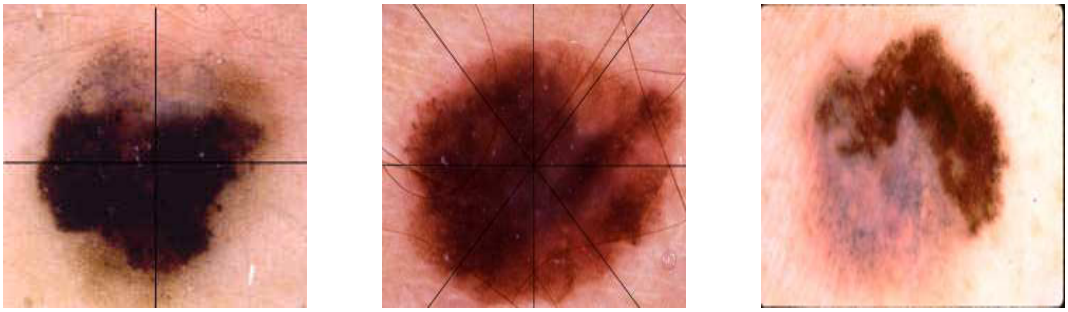

(a) (b) (c)

Figure 1. Asymmetry Border Color Features; (a) Asymmetry Test, (b) Border Test, (c) Color variegation (source: (7))

The *Menzies* method looks for negative features (Symmetry of pattern, Presence of a single color) and positive (Blue-white veil, Multiple brown dots, Pseudopods, Radial streaming, Scar-like depigmentation, Peripheral black dots/globules, Multiple (5-6) colors, Multiple blue/gray dots, Broadened network).

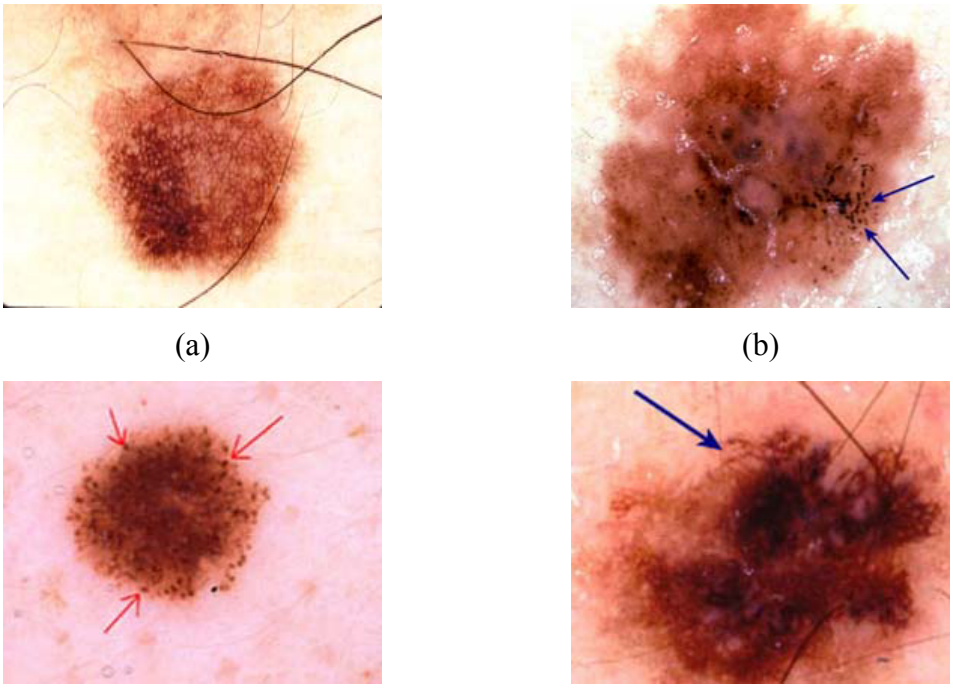

(a) (b)

(c) (d)

Figure 2. Differential Structures; (a) Pigmented network, (b) Dots, (c) Brown globules, (d) Branched streaks (source: (7))

The 7-point checklist seeks for Atypical pigment network, Blue-whitish veil, Atypical vascular pattern, Irregular streaks, Irregular dots/globules, Irregular blotches, Regression structures.

The researchers that seek to identify automatically malignant melanoma exploit the available computational capabilities by searching for many of the above, as well as, for additional features. The main features used for skin lesion image analysis are summarized bellow:

Asymmetry features

The *asymmetry* is examined with respect to a point, one or more axes. The asymmetry index is computed by first finding the principal axes of inertia of the tumor shape in the image and it is obtained by overlapping the two halves of the tumor along the principal axes of inertia and dividing the non-overlapping area differences of the two halves by the total area of the tumor.

Border Features

The most popular *border* features are the Greatest Diameter, the Area, the Border Irregularity, the Thinness Ratio (32) , the Circularity index and the variance of the

distance of the border lesion points from the centroid location (34). Apart from regarding the border as a contour, emphasis is also placed on the features that quantify the transition from the lesion to the skin. Such features are the minimum, maximum, average and variance responses of the gradient operator, applied on the intesity image along the lesion border.

Color Features

Typical color images consist of the three-color channels RGB (red, green and blue). The color features are based on measurements on these color channels or other color channels such as CMY (Cyan, Magenta, Yellow), HSV (Hue, Saturation, Value), YUV (Y-luminance, U-V chrominance components) or various combinations of them, linear or not. Color variegation may be calculated by measuring minimum, maximum, average and standard deviations of the selected channel values and by measuring chromatic differences inside the lesion (7).

Differential structures

The differential structures as described in the ABCD method, as well as most of the patterns that are used by the pattern analysis, the Menzies method and the 7-points checklist are very rarely used for automated skin lesion classification, obviously due to their complexity.

2.3 Computational methods for skin lesion classification

In this section we will examine the most popular methods for skin lesion classification. The task involves mainly three phases: feature selection, learning and testing (7), which are analyzed in the following.

The success of image recognition depends on the correct selection of the features used for the classification. This is a typical optimization problem, which may be resolved with heuristic strategies, greedy or genetic algorithms or other computational intelligence methods (9). The use of feature selection algorithms is motivated by computational reasons and by a peaking phenomenon often observed when classifiers are trained with a limited set of training samples. If the number of features is increased the classification rate of the classifiers decreases after a peak (10), (11).

During the learning phase typical feature values are extracted from a sequence of digital images representing classified skin lesions. The most classical recognition paradigm is statistical (12). Covariance matrices are computed for the discriminative measures, usually under the multivariate Gaussian assumption. Parametric

discriminant functions are then determined, allowing classification of unknown lesions (discriminant analysis). The major problem of this approach is the need for large training samples.

Neural networks are networks of interconnected nodes composed of various stages that emulate some of the observed properties of biological nervous systems and draw on the analogies of adaptive biological learning. Learning occurs through training over a large set of data where the training algorithm iteratively adjusts the connection weights (synapses), by minimizing a given error function (15), (16). Popular choices for the error function in skin lesion image classification are the Euclidean Distance or the ratio deviation defined as follows:

$$E = \sqrt{\sum_i (x_i - \bar{x})^2}\ ,\ E = \sum_i \left| 1 - \frac{x_i}{\bar{x}} \right| \qquad \text{(Equation 1)}$$

where x_i is the ith sample and $\bar{x}$ is the population mean (13).

The Support Vector Machines (SVMs) is a popular algorithm for data classification into two classes (14) (17), (18). SVMs allow the expansion of the information provided by a training data set as a linear combination of a subset of the data in the training set (support vectors). These vectors locate a hypersurface that separates the input data with a very good degree of generalization. The SVM algorithm is based on training, testing and performance evaluation, which are common steps in every learning procedure. Training involves optimization of a convex cost function where there are no local minima to complicate the learning process. Testing is based on the model evaluation using the support vectors to classify a test data set. Performance evaluation is based on error rate determination as test set data size tends to infinity.

3. Results

The development of computer-based systems for the characterization of skin images preoccupies many biomedical laboratories (33). The work in (15), (19) identified succesfully tumor, crust, hair, scale, shiny and ulcer by using features vectors. The average success rates were 85% with the chromaticity coordinates to overpass in performance the remaining color spaces. Of course it is expected that a combination of color spaces will result in a better identification. The same team used neural networks to identify variagated coloring in skin tumors with 89% correct results (15).

In (20) the CIELAB color space for the analysis of skin erythema was used. This research was conducted to test the effect of specified drugs to the human skin. In (21) a method based on feature extraction is proposed for the objective assesment of burn scars. The results illustrated the ability to objectively detect differences in skin elasticity between normal and abnormal tissue. RGB and the HIS color planes are also used for the detection of melanoma (22), showing that the use of both color planes had better results than each one seperately. The same feature extraction techniques are used even for skin images obtained by microscope with good results (23). The results from the computer based system were compared with the results from traditional methods and the mean absolute difference was about 5%.

Several efforts also concern the kinetics of skin lesions. In (24) the HIS color coordinates were used for the evaluation of wound status. The same color space in adition to the RGB values is used in (25) for the monitoring of healing processes with the introduction of ratio of variances RV. This ratio is proposed by (26) and has been used to compare together several color indexes. RV is defined as

$$RV = \frac{SD_{B^2}}{SD_{B^2} + SD_{I^2} + SD_{A^2}} \qquad \text{(Equation 2)}$$

SD_B^2 (Standard Deviation Between Days) is between day variance of the color variable computed using the mean values at each day of all wound sites and subjects.

SD_I^2 (Standard Deviation Intra Day) is the intra day variance of the color variable estimated from the computations at each day of all wound sites and subjects.

SD_A^2 (Standard Deviation Analytical) is the variance of the color variable computed using normal skin sites of all subjects and times.

Another significant application of computer supported lesion image analysis is the implementation of systems based on images produced from the fluorescence of human skin in the non visible spectra, such as infrared or ultraviolet. The feature, which is used for identification in these systems, is the intensity of the fluorescence. The first attempt on using fluorescence methods for in situ detection of melanoma was made in (27), where autofluorescence of skin tissues was excited in vivo with ultraviolet light and recorded the spectra of light emitted by healthy tissues, naevi and melanomas. It was found that melanomas generated specific patterns of variation in the fluorescence intensity, specifically local maxima in the transition zone between the melanoma and the healthy skin were detected, which was not found for naevi.

Bono and others implemented an image analysis system base on imaging of pigmented skin lesions in infrared (28). The results were very promising with 77% of lesions correctly diagnosed against 81% of correct clinical diagnoses. In (29) the ratio Imax/Imin was used where Imax and Imin are the maximum and minimum value of fluorescence intensity in regions located up to 40 mm from the lesions. This ratio had average values 14.3 for melanoma, 5.7 for naevi and 6.1 for other skin lesions. Similar techniques are described in (30) and (31) for the infrared imaging. The above described methods are sumarized in Table 1.

Reference	**Detection goal**	**Installation type**	**Visual Features**	**Classification method**	**Success rates**
(15), (19)	Tumor, crust, hair, scale, shiny ulcer of skin lesions	Video RGB Camera	Color (chromaticity) coordinates (more)	Neural networks	85-89% in average
(20)	Skin erythema	Video RGB Camera	Color - CIE L*a*b* color space	Statistical	Monitoring indexes for Follow ups
(21)	Burn scars	Video RGB Camera	Image Intensity, Skin Elasticity	Finite element analysis,	Monitoring indexes for Follow ups
(22)	Melanoma Recognition	Video RGB Camera	Color in RGB and HIS (more)	Statistical	5% deviation from manual diagnosis
(23)	Melanoma Recognition	Tissue microscopy	Epidermal and dermal features (epidermis volume, thickness, dermal epidermal junction ratio, cellular and collagen densities)	Statistical	Difference in epidermal features was 5.33% , for dermal features it was 2.76%
(25)	Wound Healing	CCD Camera	Ratio of variances, in HIS and RGB	Healing indexes measuring, the wound area and the wound color.	Monitoring indexes for Follow ups
(27)	Melanoma Recognition	In situ, ultraviolet illumination	Auto fluorescence of skin tissues	Statistical	77% (81% manual diagnoses)
(29)	Melanoma Recognition	Ultraviolet illumination	Imax/Imin, (fluorescence intensity)	Statistical	Sensitivity of 82.5%, specificity of 78.6% positive predictive value of 58.9% (Average values 14.3 for melanoma, 5.7 for naevi and 6.1 for other skin lesions)
(30), (31)	Tissue Classificatio n	Infrared illumination	Imax/Imin, (fluorescence intensity)	Statistical, Fuzzy C-means clustering	
(33)	Melanoma Recognition	Epiluminescence microscopy (ELM)	RGB/HIS/Border	Statistical (k-nearest-neighbor)	sensitivity of 87% and a specificity of 92%

Table 1. Computer-based systems for the characterization of digital skin images

Our study focused on constructing a classification system for skin lesions, enabling the distinction of malignant melanoma from dysplastic nevus. Three groups of data were considered. The first group (denoted VGP-Vertical Growth Phase) consists of cases of malignant melanoma, with measurements taken on the entire extent of the lesion. The second group (RGP-Radial Growth Phase) also refers to the malignant melanomas, but measurements are restricted to the dark area of the melanoma. The third group (DSP-Dysplastic) comprises cases of dysplastic nevus (see Figure 3).

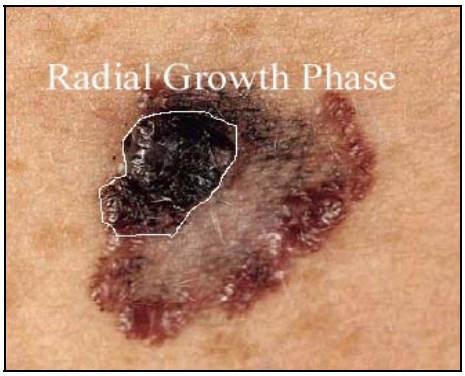

Figure 3. The RGP phase of melanoma is the circled area

Separate analyses were carried out, one between VGP and DSP, and the other between RGP and DSP. Both comparisons are made by linear discriminant analysis , by fitting a neural network model and by utilizing the SVM algorithm.

VGP-DSP Comparison

A training data set of 34 cases at the Dept of Plastic Surgery and Dermatology in Athens General Hospital Dept of Plastic Surgery and Dermatology in Athens General Hospital collected within a period of 6 months. The total number of lesions captured was: 14 melanomas and 20 dysplastic naevi. The mean thickness of melanomas lesions was measured after biopsy at approximately 1.5 mm penetration through the skin.

The sensitivity and specificity rates using discriminant analysis, neural networks and support vector machines are presented in Table 2 and Table 3 for VGP-DSP and RGP-DSP classification. We have used the cross-validation or ëleaving-one-outí estimator of the rate of correct classifications, obtained by seeing how each observation is classified according to a function recalculated after omitting that observation from the analysis. The neural networks models also performed very well.

Using four principal components as input, the success rate achieved was 97% (93% of VGP and 100% of DSP). This was reduced to 85% correct classification (79% of VGP and 90% of DSP) using only the first two principal components. Using Greatest Diameter and Thinness Ratio as features (32) for input ñ that is, the two significant predictors identified by the discriminant analysis method ñ gave 97% correct classification, exactly as in the discriminant analysis. The corresponding sensitivity and specificity indexes are presented in Table 2.

Method	**Total correct classification**	**Sensitivity**	**Specificity**
Discriminant Analysis using 4 Features	33/34 or 97%	93%	100%
Discriminant Analysis using 2 Features as the most significant for discrimination	32/34 or 94%	86%	100%
Neural Networks using four principal components as input	33/34 or 97%	93%	100%
Neural Networks using two principal components as input	29/34 or 85%	79%	90%
SVM (Gaussian RBF Kernel, sigma=4, 7 support vectors	94% 32/34	86%	100%

Table 2 . Sensitivity and Specificity Indexes of the VGP - DSP classification

Regarding the SVM algorithm, different polynomial kernel functions were tried on subsets of the 34 cases, in order to find the less complex kernel function that results in low number of support vectors comparing to the train set. The support vectors calculated using the Gaussian radial base kernel function were the fewest with 100% successful classification of the test data set. These support vectors were tested using all the cases of malignant melanoma denoted as VGP and dysplastic nevus denoted as DSP and it performed excellently, classifying them correctly 94%.

RGP-DSP Comparison

The discriminant analysis method has been applied to the problem of RGP-DSP comparison and classified correctly 97% of the cases (100% of DSP and 93% of RGP). The neural network model achieved 100% correct classification taking four principal components as input and 94% correct (100% of DSP and 86% of RGP) using two components. Taking as input the three variables that had been selected by

the discriminant analysis procedure, the neural network again gave 100% correct classification. The results are depicted in Table 3.

Method	Total correct classification	Sensitivity	Specificity
Discriminant Analysis using 4 Features	33/34 or 97%	93%	100%
Discriminant Analysis using 2 Features as the most significant for discrimination	30/34 or 88%	86%	100%
Neural Networks using four principal components as input	34/34 or 100%	100%	100%
Neural Networks using two principal components as input	32/34 or 94%	86%	90%
SVM (First order polynomial kernels, 5 support vectors)	97%	93%	100%

Table 3 Sensitivity and Specificity Indexes of the RGP - DSP classification

For the SVM classification a first order polynomial was used and 5 support vectors were calculated. These support vectors were tested using all the cases of malignant melanoma denoted as RGP and dysplastic nevus denoted as DSP and it performed very well, classifying correctly 97% of the cases.

4. Conclusions

The most remarkable systems for the automated detection of malignant melanoma have been surveyed. These systems employ a variety of methods for the image acquisition, the feature definition and extraction as well as the lesion classification from features.

The most promising image acquisition techniques appear to be those that reveal the skin structure through selected spectral images. However, the problem of repeatability of the measurements for follow-up studies has not been satisfactorily resolved.

Regarding the features, it is clear that the emphasis has been on assessment of lesion size, shape, color, and texture. These statistical parameters were chosen primarily for computational convenience; they can be acquired with well-established analytic techniques at a manageable computational cost. However, they do not correspond to known biological phenomena and do not model human interpretation of dermoscopic imagery. On the contrary, the structural patterns that are considered essential for manual lesion categorization seem to have been neglected by the

computational intelligence community, due to their complexity, although their exploitation could provide crucial information.

As far as the classification method is concerned, the SVM seems to perform better. However, it is actually the selected features that are critical for the performance of the classifier and the training procedure as well, which has to include the biggest possible variety of cases.

The results presented so far, from the research community are promising for the future. It is now necessary to examine more patients in order to increase the number of cases, particularly during the classification phase. This will clarify the issue of selecting the most powerful variables for classification and may also enable even better classification if examination of the differences in results between the two methods casts light on why misclassifications can arise.

References

(1) Marks R. Epidemiology of melanoma. Clin Exp Dermatol 2000;25:459ñ63.

(2) Moncrieff M, Cotton S, Claridge E, Hall P (2002) Spectrophotometric intracutaneous analysis - a new technique for imaging pigmented skin lesions. British Journal of Dermatology 146(3), 448-457

(3) Loane M., Gore H., Corbet R., Steele K., ìEffect of Camera performance on diagnostic accuracyî, Journal of Telemedicine and Telecare, 3, pp. 83-88, 1997.

(4) I. Maglogiannis, D. Kosmopoulos : "A System for the Acquisition of Reproducible Digital Skin Lesion Images" Technology and Healthcare, IOS Press 11 (2003) 425-441

(5) Gutenev A., Skladnev V. N., Varvel D., ìAcquisition-time image quality control in digital dermatoscopy of skin lesionsî, Computerized Medical Imaging and Graphics, 25, pp.495-499, 2001.

(6) Giuseppe Argenziano et al, Dermoscopy of pigmented skin lesions: Results of a consensus meeting via the Internet, J AM ACAD DERMATOL ,VOLUME 48, NUMBER 5, p. 680-693, 2003

(7) Electronic available information at Skin Oncology Teaching Center http://www.dermoncology.com/

(8) I. Maglogiannis, C. Caroni, S. Pavlopoulos, V. Karioti, ì Utilizing Artificial Intelligence for the Characterization of Dermatological Imagesî, 4th International Conference ìNeural Networks and Expert Systems in Medicine and Healthcareî, NNESMED, pp 362-368, Greece 2001

(9) H. Handels, Th. Rofl, J. Kreusch, H. H. Wolff and S. J. Pˆppl : ìFeature selection for optimized skin tumor recognition using genetic algorithmsî Artificial Inteligence in Medicine 16 283-297 1999

(10) Jain A.K. ìAdvances in statistical pattern recognition. In: P.A. Devijer and J. Kittler Editorsî, Pattern recognition, theory and applications Springer, Berlin (1986).

(11) A.K. Jain and W.G. Waller ìOn the optimal number of features in the classification of multivariate gaussian dataî Pattern Recogn. 10 (1978), pp. 365Ø374.

(12) Duda R.O., Hart P. E. ìPattern classification and skin analysisî New York , John Willey 1973

(13) A. Jain, R. Dubes : ìAlgorithms for clustering dataî Prentice Hall Englewood Cliffs NJ 1988

(14) Burges C: A tutorial on support vector machines for pattern recognition [http://www.kernel-machines.org/].

(15) Scott E Umbaugh, Randy H. Moss, William V. Stoecker : "Applying Artificial Intelligence to the identification of Variegated Coloring in Skin Tumors", IEEE Engineering in Medicine and Biology Magazine , December 1991, pp. 57-62.

(16) Ajaya. Durg, William V. Stoecker, John P. Vookson, Scott E Umbaugh, Randy H. Moss : " Identification of Variegated Coloring in Skin Tumors ", IEEE Engineering in Medicine and Biology Magazine , September 1993, pp. 71-75.

(17) Christianini N, Shawe-Taylor J: An introduction to support vector machines. Cambridge University Press, 2000.

(18) Schˆ lkopf B: Statistical learning and kernel methods. [http://research.Microsoft.com/~bsc].

(19) S. Umbaugh, Y. Wei, M. Zuke : ìFeature Extraction in Image Analysisî IEEE Engineering in Medicine and Biology pp 62-73 Jul/Aug 1997

(20) M. Nischic and C. Forster : ìAnalysis of Skin Erythema using true color imagesî IEEE Transactions on Medical Imaging Vol 16 No 6 December 1997

(21) L. Tsap, D. Goldgof, S. Sarkar, P. Powers : ìVision-based tecnique for objective assesment of burn scarsî IEEE Transactions on Medical Imaging vol17, pp 620-633 1998

(22) S. Tomatis, C Bartol, G. Tragni, B. Farina, R. Marchesini : ìImage analysis in the RGB and HS colour planes for a computer assisted diagnosis of cutaneous pigmented lesionsî Tumori vol 84 pp 29-32 1998

(23) J. Sanders B. Goldstein, D. Leotta K. Richards : ìImage proccesing tecniques for quantitative analysis of skin structuresî Computer Methods and Programs in Biomedicine 59 pp 167-180 1999

(24) G. Hansen, E. Sparrow, J. Kokate, K. Leland, P. Iaizzo : ìWound Status Evaluation Using Color Image Processingî IEEE Transactions on Medical Imaging, vol16, no1 pp 78-86 Feb 1997

(25) M. Herbin, F. Bon, A. Venot, F. Jeanlouis, M. Dubertret, L. Dubertret, G. Strauch : ìAssessment of Healing Kinetics Through True Color Image Processingî IEEE Transactions on Medical Imaging, vol12, no1 pp 39-43 Mar 1993

(26) S. Chin : ìThe assessment of methods of measurementsî Stat. Med. Vol.9 pp 351-362, 1990.

(27) W. Lohman, E. Paul : ìIn situ detection of melanomas by fluorescence measurementsî Naturewissenschaften 1988, 75 201-202

(28) Bono, S. Tomatis, C. Bartoli : ìThe invisible colors of melanoma. A telespectrophotometric diagnostic approach on pigmented skin lesionsî European Journal of Cancer 1996 32A, 727-729.

(29) B. W. Chwirot, S. Chwirot, J. Redziski and Z. Michniewicz : ìDetection of melanomas by digital imaging of spectrally resolved ultraviolet light-induced autofluorescence of human skinî European Journal of Cancer October 1998 34, 1730-1734

(30) J. Mansfield, M. Sowa, J. Payette, B. Abdulrauf, M. Stranc, H. Mantsch : ìTissue viability by multispectral near infrared imaging : A fuzzy C-means clustering analysisî IEEE Transactions on Medical Imaging vol 17, 6, pp 1011-1018 1998

(31) B. Jones ìReappraisal of the use of infrared thermal image analysis in medicineî IEEE Transactions on Medical Imaging vol 17, 6, pp 1019-1027 1998

(32) I. Maglogiannis, E. Zafiropoulos: ìUtilizing Support Vector Machines For The Characterization of Digital Medical Imagesî BMC Medical Informatics and Decision Making 2004, 4:4

(33) H. Ganster, P. Pinz, R. Rohrer, E. Wildling, M. Binder, H. Kittler, ìAutomated melanoma recognitionî, IEEE Transactions on Medical Imaging, 20 (3), Mar 2001 233 -239

(34) A. Bono, S. Tomatis, C. Bartoli, G. Tragni, G. Radaelli, A. Maurichi, and R. Marchesini. The ABCD system of melanoma detection: A spectrophotometric analysis of the asymmetry, border, color, and dimension. *Cancer* **85**(1), 1999, p. 72-77.

LIST OF FIGURES

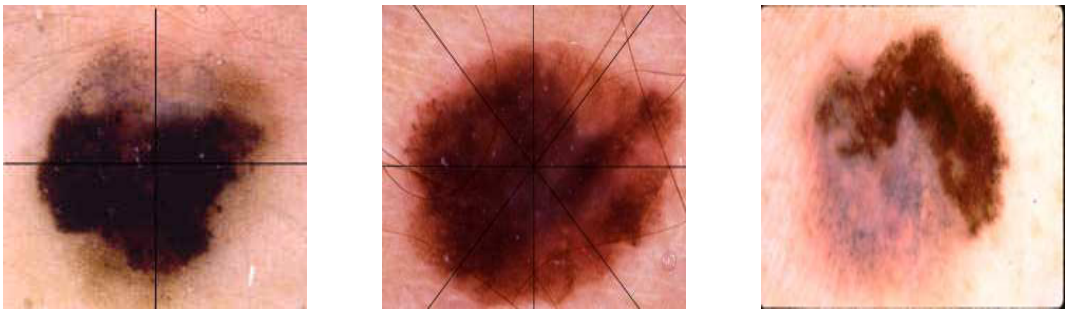

(a) (b) (c)

Figure 1. Asymmetry Border Color Features; (a) Asymmetry Test, (b) Border Test, (c) Color variegation (source: (7))

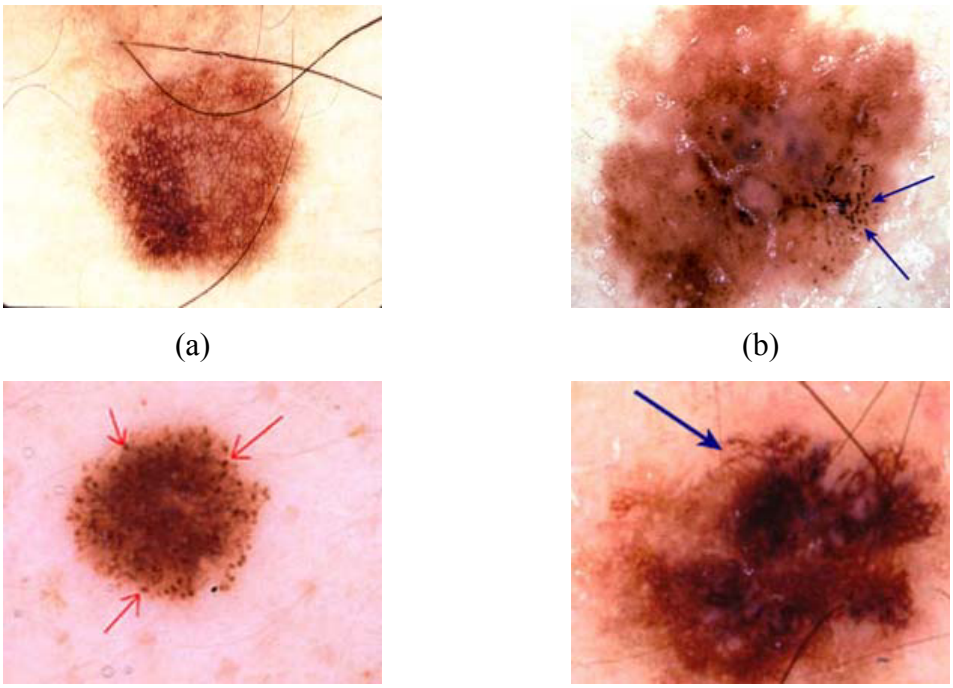

(a) (b)

(c) (d)

Figure 2. Differential Structures; (a) Pigmented network, (b) Dots, (c) Brown globules, (d) Branched streaks (source: (7))

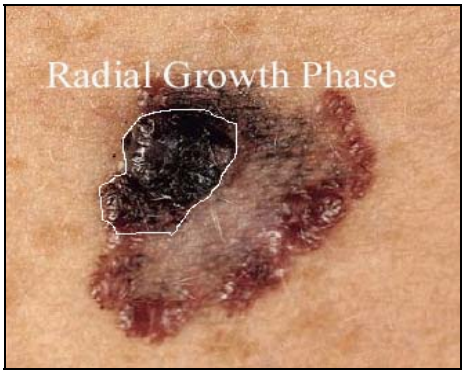

Figure 3. The RGP phase of melanoma is the circled area

LIST OF TABLES

Reference	Detection goal	Installation type	Visual Features	Classification method	Success rates	Comments
(15), (19)	Tumor, crust, hair, scale, shiny ulcer of skin lesions	Video RGB Camera	Color (chromaticity) coordinates (more)	Neural networks	85-89% in average	
(20)	Skin erythema	Video RGB Camera	Color - CIE L*a*b* color space	Statistical		
(21)	Burn scars	Video RGB Camera	Image Intensity, Skin Elasticity	Finite element analysis,		
(22)	Melanoma Recognition	Video RGB Camera	Color in RGB and HIS (more)	Statistical	5% deviation from manual diagnosis	
(23)	Melanoma Recognition	Tissue microscopy	Epidermal and dermal features (epidermis volume, thickness, dermal epidermal junction ratio, cellular and collagen densities)	Statistical	Difference in epidermal features was 5.33% , for dermal features it was 2.76%	
(25)	Wound Healing	CCD Camera	Ratio of variances, in HIS and RGB	Healing indexes measuring, the wound area and the wound color.		Follow-up studies
(27)	Melanoma Recognition	In situ, ultraviolet illumination	Autofluorescence of skin tissues	Statistical	77%	81% manual diagnoses
(29)	Melanoma Recognition	Ultraviolet illumination	Imax/Imin, (fluorescence intensity)	Statistical	Sensitivity of 82.5%, specificity of 78.6% positive predictive value of 58.9%	Average values 14.3 for melanoma, 5.7 for naevi and 6.1 for other skin lesions
(30), (31)	Tissue Classificatio n	Infrared illumination	Imax/Imin, (fluorescence intensity)	Statistical, Fuzzy C-means clustering		
(33)	Melanoma Recognition	Epiluminescence microscopy (ELM)	RGB/HIS/Border	Statistical (k-nearest-neighbor)	sensitivity of 87% and a specificity of 92%	

Table 4. Computer-based systems for the characterization of digital skin images

Method	Total correct classification	Sensitivity	Specificity
Discriminant Analysis using 4 Features (which functions?, which features)	33/34 or 97%	93%	100%
Discriminant Analysis using 2 Features as the most significant for discrimination (which functions?, which features)	32/34 or 94%	86%	100%
Neural Networks using four principal components as input	33/34 or 97%	93%	100%
Neural Networks using two principal components as input	29/34 or 85%	79%	90%
SVM (Gaussian RBF Kernel, sigma=4, 7 support vectors	94% 32/34	86%	100%

Table 5 . Sensitivity and Specificity Indexes of the VGP - DSP classification

Method	Total correct classification	Sensitivity	Specificity
Discriminant Analysis using 4 Features	33/34 or 97%	93%	100%
Discriminant Analysis using 2 Features as the most significant for discrimination	30/34 or 88%	86%	100%
Neural Networks using four principal components as input	34/34 or 100%	100%	100%
Neural Networks using two principal components as input	32/34 or 94%	86%	90%
SVM (First order polynomial kernels, 5 support vectors)	97%	93%	100%

Table 6 Sensitivity and Specificity Indexes of the RGP - DSP classification